Chem Soc Rev

TUTORIAL REVIEW

View Article Online
View Journal

Cite this: DOI: 10.1039/d1cs00358e

Emerging contrast agents for multispectral optoacoustic imaging and their biomedical applications†

Yinglong Wu, [ab] Fang Zeng, [a] Yanli Zhao *[b] and Shuizhu Wu *[a]

Optoacoustic imaging is a hybrid biomedical imaging modality which collects ultrasound waves generated *via* photoexciting contrast agents in tissues and produces images of high resolution and penetration depth. As a functional optoacoustic imaging technique, multispectral optoacoustic imaging, which can discriminate optoacoustic signals from different contrast agents by illuminating samples with multi-wavelength lasers and then processing the collected data with specific algorithms, assists in the identification of a specific contrast agent in target tissues and enables simultaneous molecular and physiological imaging. Moreover, multispectral optoacoustic imaging can also generate three-dimensional images for biological tissues/samples with high resolution and thus holds great potential in biomedical applications. Contrast agents play essential roles in optoacoustic imaging, and they have been widely explored and applied as probes and sensors in recent years, leading to the emergence of a variety of new contrast agents. In this review, we aim to summarize the latest advances in emerging contrast agents, especially the activatable ones which can respond to specific biological stimuli, as well as their preclinical and clinical applications. We highlight their design strategies, discuss the challenges and prospects in multispectral optoacoustic imaging, and outline the possibility of applying it in clinical translation and public health services using synthetic contrast agents.

Received 13th April 2021

DOI: 10.1039/d1cs00358e

rsc.li/chem-soc-rev

Key learning points

(1) General concept of multispectral optoacoustic imaging and the significance of contrast agents for biomedical applications.
(2) Introduction to the multispectral optoacoustic imaging system and the photophysical, chemical and biological properties of contrast agents.
(3) Advances in contrast agents and their preclinical applications with multispectral optoacoustic imaging.
(4) Recent progress in clinical applications using multispectral optoacoustic imaging.
(5) Perspectives and potential challenges in multispectral optoacoustic imaging and the development of contrast agents for future research and clinical translation.

1. Introduction

Biomedical imaging is a non-invasive approach to the visualization and quantification of biological activities and is frequently utilized to diagnose, predict, stage and monitor the development of diseases. With the continuous evolution of computing power, the current imaging techniques can provide multiscale visualization from molecules to cells, organs, tissues, and the whole organism. Moreover, a library of tools dedicated to imaging has emerged over the past few decades and enables clear delineation of the anatomical structure, morphology, and physiological functions at the above-mentioned different scales by generating two-dimensional (2D) or three-dimensional (3D) images, which allow us to understand and examine the medical conditions of patients.[1] As one important imaging modality, optical imaging (*e.g.* fluorescence imaging) has been widely employed in medical diagnosis and preclinical research because it can significantly avoid exposure of patients to harmful ionizing radiation using visible or near-infrared light sources.[2] However, the strong light scattering in biological

[a] State Key Laboratory of Luminescent Materials and Devices, Guangdong Provincial Key Laboratory of Luminescence from Molecular Aggregates, College of Materials Science and Engineering, South China University of Technology, Wushan Road 381, Guangzhou, 510640, China. E-mail: shzhwu@scut.edu.cn
[b] Division of Chemistry and Biological Chemistry, School of Physical and Mathematical Sciences, Nanyang Technological University, 21 Nanyang Link, Singapore, 637371, Singapore. E-mail: zhaoyanli@ntu.edu.sg

† Electronic supplementary information (ESI) available. See DOI: 10.1039/d1cs00358e

tissues compromises the spatial resolution and penetration depth of optical imaging, and thus greatly limits its clinical applications.[3]

Optoacoustic (OA, also referred to as photoacoustic) imaging is an emerging non-invasive biomedical imaging modality based on a so-called ''light-in & sound-out'' approach. An optoacoustic system delivers light energy to tissues, detects ultrasound waves generated by the contrast agents in the tissues as a result of thermoelastic expansion, and generates optoacoustic images from the collected acoustic data. It integrates the beneficial advantages of both optical imaging and ultrasound imaging, featuring excellent contrast, high resolution (down to several micrometres) and deep tissue penetration (from several millimetres to centimetres).[4]

However, despite these excellent characteristics, optoacoustic imaging at a single excitation wavelength cannot discriminate signals from different contrast agents (absorbers) in tissues, since each absorber generates its own signal, and the overlapping optoacoustic signals from multiple absorbers make it difficult to accurately detect the analyte of interest.

To address this issue, a multispectral (or multiwavelength) optoacoustic imaging technique has been designed to sequentially irradiate a sample with a pulsed laser of multiple wavelengths and then perform spectral processing using unmixing algorithms.[5] Multispectral optoacoustic imaging can discriminate the ultrasound signals from different contrast agents in tissues, thus the distribution and level of each contrast agent in the tissues can be visualized and quantified separately. Over the past several years, this technique has been evolving rapidly, leading to a variety of exciting discoveries and applications.

Parallel to the exciting progress in this imaging technique, considerable efforts have been made to develop functional

Yinglong Wu

Yinglong Wu received his BEng degree in Materials Science and Engineering from the South China University of Technology in 2014, and then received his PhD degree in Materials Science from the South China University of Technology in 2018 under the mentorship of Prof. Shuizhu Wu. Currently, he is working as a postdoctoral research fellow at the School of Physical and Mathematical Sciences, Nanyang Technological University (NTU) under the supervision of Prof. Yanli Zhao. His research interests include design and development of organic materials for applications in biosensing, bioimaging and drug delivery.

Fang Zeng

Fang Zeng received his BEng degree and MS degree in Polymer Materials from Chengdu University of Science and Technology and Tianjin University, respectively. He received his PhD degree in Materials Science and Engineering from the South China University of Technology (SCUT) under a joint PhD program of SCUT and Osaka University with Prof. Zhen Tong and Prof. Takahiro Sato. He is currently professor of materials science at SCUT, and his research interests are nanomedicines, nano-optical systems, etc.

Yanli Zhao

Yanli Zhao is currently the Lee Soo Ying Professor in Materials Chemistry at Nanyang Technological University. He received his BSc degree in Chemistry from Nankai University and his PhD degree in Physical Chemistry there under the supervision of Professor Yu Liu. He was a postdoctoral scholar with Professor Sir Fraser Stoddart at the University of California Los Angeles and subsequently at the Northwestern University. He also conducted postdoctoral research with Professor Jeffrey Zink at the University of California Los Angeles. His current research is focused on integrated nanosystems for theranostics, and porous materials for gas storage and catalysis.

Shuizhu Wu

Shuizhu Wu is currently professor of materials science at the South China University of Technology (SCUT). She received her BEng degree and MS degree in Polymer Materials from Tianjin University and PhD degree in Materials Science from SCUT. During her career, she has been awarded the National Science Fund for Distinguished Young Scholars (NSFC) and appointed as ''Distinguished Professor of Guangdong Province''. Her research activities include design and synthesis of fluorescent compounds, photophysical systems, nanoparticle-based fluorescence sensing and imaging systems, biomaterials and others.

contrast agents, which play critical roles in multispectral optoacoustic imaging.[6] The chromophores with absorption spectra that exhibit characteristic differences from those of background tissues are best suited for multispectral optoacoustic imaging as contrast agents. Among the contrast agents, the activatable ones which can respond to specific biological stimuli and thus elicit changes in optoacoustic signals are particularly advantageous due to their salient properties, such as the high signal-to-noise ratio (SNR), real-time correlation between optoacoustic signals and disease condition, and probe-concentration-independent contrast, hence the imaging sensitivity can be further improved.[7] With the aid of rationally designed contrast agents, especially the activatable ones, multispectral optoacoustic imaging could be brought into full play in biomedical applications, including disease diagnosis, disease progression monitoring and therapy assessment (Scheme 1).

To date, a great number of optoacoustic contrast agents (probes) have been developed and used in biomedical imaging, and several excellent reviews related to contrast agents have been published.[6–13] However, due to the fast evolution of multispectral optoacoustic imaging, many new contrast agents, especially the activatable ones, have emerged in the last few years and are yet to be reviewed. In addition, recent progress in clinical practice with multispectral optoacoustic imaging should also be summarized to highlight the application of this imaging technique. This review outlines the latest advances in emerging contrast agents and their biomedical applications using a multispectral optoacoustic imaging technique. We introduce the photophysical, chemical and biological properties of available contrast agents, and highlight the development of contrast agents reported in the last few years. We also discuss their preclinical and clinical applications and emphasize the design strategies of activatable contrast agents for multispectral optoacoustic imaging. Finally, conclusions and outlook are given to further stimulate research interest in the development of new robust contrast agents, to explore broader biomedical applications and promote clinical translation and public health service of multispectral optoacoustic imaging.

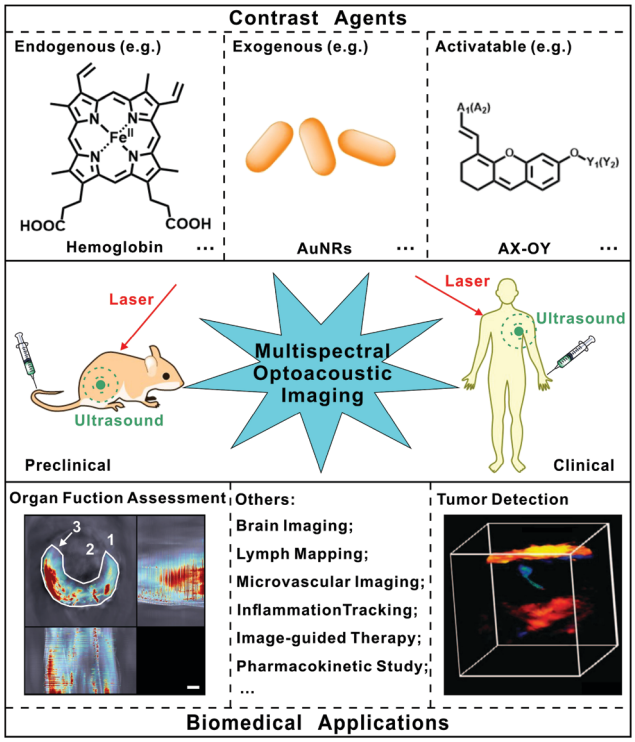

Scheme 1 Schematic illustration of contrast agents for multispectral optoacoustic imaging and their biomedical applications. Organ labeling: (1) spinal cord; (2) aorta; (3) liver. The liver injury region is manifested by an optoacoustic signal (shown in color) from the activated contrast agent. This figure has been adapted/reproduced from ref. 61 with permission from Springer Nature copyright 2018 and from ref. 79 with permission from the American Association for the Advancement of Science copyright 2015.

2. Brief introduction to instrumentation for multispectral optoacoustic imaging and photophysical, chemical and biological properties of contrast agents

Generally, an optoacoustic imaging system consists of three main components: (1) a light source (mostly a pulsed laser) with illumination optics, which delivers light energy to the tissue of interest; (2) one or an array of ultrasound detector(s) measuring the generated acoustic signals, and (3) a signal processing and reconstruction unit which produces final images.[14] To achieve multispectral imaging, a wavelength-tuning laser source and supporting spectral unmixing algorithms should be adopted to separate individual signals from multiple absorbers in tissues.[5] Currently, several companies have developed commercially available multispectral optoacoustic imaging systems for biomedical imaging, and their technologies, specifications, as well as some characteristics are listed and compared in Table S1 (ESI†).

Furthermore, to realize tomographic imaging, which is a non-invasive imaging technique that allows for the visualization of the internal structures of an object in a "slice-by-slice" manner, scanning techniques with high repetition rate lasers, and rapid data transfer from the acquisition electronics to the reconstruction unit, and fast image reconstruction techniques have been developed to produce 2D cross-sectional images.[15–17]

The tomographic imaging can provide 3D images by using stacks of 2D cross-sectional images. On the other hand, 3D images can also be directly obtained with various detector arrays.[16] In particular, a handheld 3D detector system has been developed with a compact detector and a fast-tunable laser,[17] and its acquired images can comprehensively display information about biological functions or disease foci in a spatio-temporal manner, and hence it holds great potential in clinical translation.

In general, multispectral optoacoustic imaging involves the following steps (Fig. 1). First, contrast agents (both endogenous

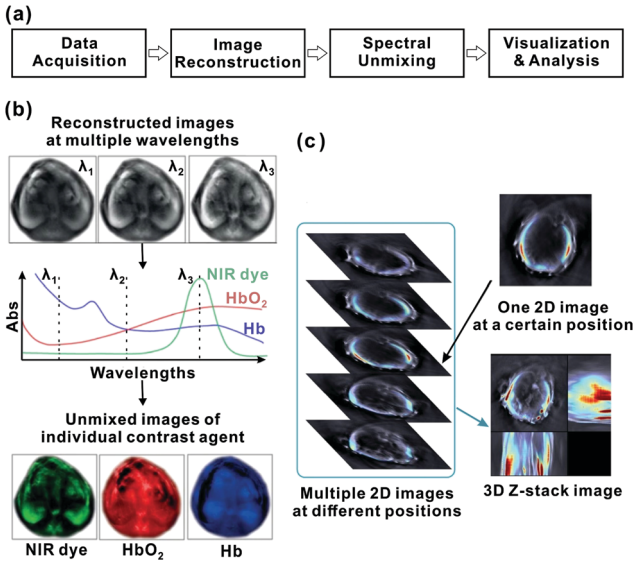

Fig. 1 (a) Operation chain of multispectral optoacoustic imaging. (b) Schematic illustration of spectral unmixing. Reproduced with permission from ref. 4. Copyright 2016 Springer Nature. (c) Schematic illustration of a 3D z-stack optoacoustic image produced by rendering 2D cross-sectional images. Reproduced from ref. 66 with permission from the American Chemical Society copyright 2019.

ones such as hemoglobin and exogenous ones such as synthetic chromophores) in biological tissues absorb the optical excitation energy from a short-pulsed laser, and then convert it to thermal energy which causes an increase in local temperature. Then, the instantaneous temperature rise induces pressure jump and generates acoustic waves at megahertz frequencies, which can be detected by broadband ultrasound detector(s) for data acquisition. For tomographic imaging, the acoustic signals collected around the illuminated sample are subjected to tomographic reconstruction using a mathematical algorithm to form optoacoustic images.[18,19] Afterwards, spectral unmixing is performed to separate the contribution of different contrast agents by using an appropriate numerical algorithm.[19,20] The image reconstruction and spectral unmixing process not only allow for quantitative analysis but also improve detection sensitivity and specificity.[5] Finally, the distribution and concentration of all contrast agents in the sample can be visualized and quantified separately in the 2D or 3D images. As the performance of contrast agents defines the quality of multispectral optoacoustic imaging and their applicability, fully understanding their photophysical, chemical and biological properties is of high importance.[6]

Given that the generated optoacoustic signal is governed by the absorption properties of contrast agents as well as the deactivation pathways of their excited states, the robust contrast agents should meet the following requirements in terms of photophysics as much as possible to improve the quality of multispectral optoacoustic imaging:[7] (1) a characteristic absorption spectrum with significant steep peak(s) in the near-infrared range (NIR) for definite identification by the spectral unmixing process even at diluted concentrations in biological tissues (because a narrow spectral profile contributes to more accurate and sensitive spectral unmixing over a broad and overlapping spectrum); (2) a high extinction coefficient for maximizing light absorption; (3) high photostability for unchanging spectral features after light irradiation; (4) high heat conversion efficiency for maximizing the conversion of light to heat and generation of strong acoustic signals; and (5) low quantum yields of competitive deactivation pathways of the excited states (*e.g.* fluorescence, phosphorescence, energy transfer, *etc.*) for minimizing energy losses.

In addition to the above-mentioned requirements on photophysics, the preferable contrast agents should also exhibit the following physical, chemical and biological properties: (1) good water solubility or dispersibility for promoting bioavailability and stability in the biosystem; (2) high chemical stability; (3) excellent biocompatibility for preventing rapid biodegradation or excretion; (4) low toxicity and immunogenicity for safe use in preclinical and clinical research; (5) passive or active targeting ability for improving accumulation at tissues of interest; and (6) activatability for biomarker-specific optoacoustic signal generation, to provide disease-specific information, minimize the influence of background noise and allow for real-time imaging of dynamic biological processes by responding to a specific stimulus of interest.

3. Endogenous contrast agents

Endogenous contrast agents (absorbers) are inherent components in biological tissues, which exhibit some distinct advantages: (1) non-toxic; (2) abundant; (3) no interference with physiological processes and (4) no complicated regulatory approvals required for clinical use. Generally, endogenous contrast agents with near-infrared absorption for optoacoustic imaging include hemoglobin, melanin, lipids, collagens and water (Fig. 2a). They could provide structural and functional information of biological tissues based on their unique spectral characteristics. Recently, many biomedical applications have been achieved by the multispectral optoacoustic imaging of endogenous contrast agents.

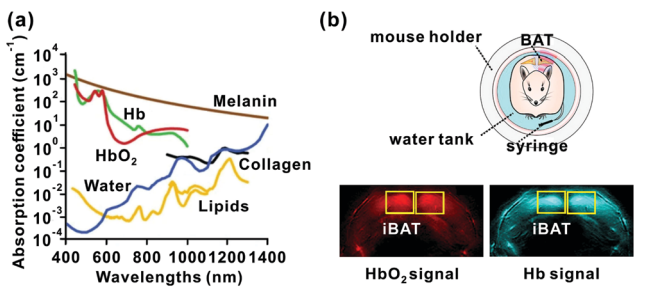

Fig. 2 (a) Absorption coefficient of the main endogenous contrast agents. Adapted from ref. 7 with permission from Springer Nature copyright 2016. (b) Schematic display for multispectral optoacoustic imaging of brown adipose fat in mice and the resulting images for HbO_2 and Hb after spectral unmixing. This figure has been adapted/reproduced from ref. 26 with permission from Elsevier copyright 2019.

3.1 Hemoglobin

Hemoglobin, a functional protein in organisms, plays a critical role in oxygen delivery throughout the body and maintains a homeostatic balance between oxyhemoglobin (HbO_2) and deoxyhemoglobin (Hb). Deoxyhemoglobin undergoes structural and electronic changes and subsequent spectral alternation after binding with oxygen and being converted to oxyhemoglobin. Such a transformation makes it possible to monitor hemoglobin- or oxygen-related physiological and pathological changes (*e.g.*, blood oxygen level, tumour angiogenesis, *etc.*) by using multispectral optoacoustic imaging.

For example, Karmacharya *et al.* employed a multispectral optoacoustic imaging system to image hemoglobin in a rat model of liver fibrosis. They observed an elevated optoacoustic signal, which represents the enhanced oxygen saturation and hemoglobin concentration in the diethylnitrosamine-induced liver fibrosis. This result demonstrates the ability of multispectral optoacoustic imaging to noninvasively assess the functional physiological changes in liver tissue during the progression of liver fibrosis.[21] Moreover, by imaging endogenous Hb and HbO_2 using a multispectral optoacoustic tomography (MSOT) system, which is a commercially available multispectral optoacoustic system with a tomography imaging technique, Olefir *et al.* achieved the noninvasive mapping and decomposition of neural-dynamics and intact mouse brain organization.[22]

In another research, Costa *et al.* evaluated the baseline variability of hemoglobin and relative blood oxygen saturation (sO_2) in a mouse model of subcutaneous head and neck tumours with an MSOT system.[23] They found a negative correlation between the percent decrease in blood sO_2 and the tumour growth rate, thus providing an approach for monitoring the efficacy of cancer therapy.

3.2 Melanin

Melanin is a universal natural pigment in hair, skin and eyes, which helps protect humans from excessive exposure to harmful ultraviolet radiation due to its strong light absorption capability. Notably, melanin is produced by melanocytes, which might form malignant melanomas once mutating and growing out of control. Therefore, as an endogenous contrast agent with intense optical absorption, melanin can be exploited in the sensitive characterization of primary and metastatic melanomas by multispectral optoacoustic imaging.

For example, Lavaud *et al.* studied the melanoma metastases in mice brains by imaging endogenous melanin.[24] In the mouse model of melanoma brain metastases, an optoacoustic signal of melanin in tumour-bearing brains was found 3 times higher than the background signal in healthy brains. Moreover, the tumour angiogenesis and hypoxia were also well characterized by imaging the hemoglobin in brain tissues. In another research, Khattak *et al.* achieved the *in vivo* quantification of the dynamic growth of conjunctival melanomas with multispectral optoacoustic imaging in a non-invasive manner.[25]

3.3 Other endogenous contrast agents

Different from hemoglobin and melanin with strong absorption in the range of 650–900 nm, some other important endogenous chromophores, such as lipids, collagens and water, exhibit high absorption in the extended near-infrared region (900–1300 nm) and thus can only be tracked in the longer wavelength region. Serving as biosynthetic precursors, energy storehouses and signalling molecules, lipids are essential components in mammals. The collagens, which are found in the bones, muscles, skin and tendons, are a group of extracellular matrix proteins and the most abundant proteins. Non-invasive mapping of the distribution of these endogenous species with multispectral optoacoustic imaging can help us to investigate the initiation and progression of related diseases.

For example, Reber *et al.* studied the brown adipose tissue (BAT) activation and tissue metabolic activity through imaging the endogenous contrast agents using an MSOT system (Fig. 2b).[26] The reconstructed images of Hb, HbO_2, water and lipids revealed the morphological discrimination and tissue composition differences in the BAT and white adipose tissue, as well as the variation in BAT components between the healthy and diabetic tissues.

Crohn's disease is a chronic autoimmune disease characterized by obstructing intestinal strictures due to inflammation, fibrosis, or a combination of both. Recently, Zhu *et al.* observed significant differences in the contents of hemoglobin and collagen between the intestinal fibrosis and inflammation in a rat model with multispectral optoacoustic imaging, which displayed clinical potential to manage Crohn's disease.[27] Moreover, Yan *et al.* found that cervical remodelling could be evaluated by assessing the relative collagen and water content of the uterine cervix in a pregnant murine model with multispectral optoacoustic imaging, which is crucial for reproductive success.[28]

4. Exogenous contrast agents

Multispectral optoacoustic imaging with endogenous contrast agents has been widely studied and shown to be useful in a variety of biomedical applications. On the other hand, the oral or injectable ones, known as exogenous contrast agents, can be used to greatly enhance the imaging resolution, contrast and depth, and thus further facilitate molecular optoacoustic imaging.[4] Hence, exogenous contrast agents show significant promise in their ability to assist multispectral optoacoustic imaging in biomedical applications such as disease diagnosis, therapy planning, and monitoring of treatment outcomes. Particularly, some targeted contrast agents can provide molecular-specific information.

For a specific biomedical application by multispectral optoacoustic imaging, the background optoacoustic signals originating from the strong optical absorption of various endogenous contrast agents in tissues must be separated when utilizing exogenous contrast agents, to achieve the separate visualization of individual contrast agent. To this end, spectral unmixing

should be adopted to resolve the signals from both endogenous and exogenous contrast agents. In recent years, a variety of chromophores have been selected or developed as exogenous contrast agents for different application purposes. Some exogenous contrast agents typically have an intense absorption and high heat conversion efficiency, thus they can also be used for photothermal therapy (PTT), which utilises the photoexcitation-induced heat to trigger the death of abnormal cells.[10,29] In this section, some examples of new exogenous contrast agents for multispectral optoacoustic imaging are presented. They are classified based on their structures and functions, including molecular contrast agents, nanosized contrast agents and genetically engineered contrast agents. However, the activatable exogenous contrast agents are covered in Section 5.

4.1 Molecular contrast agents (MCAs)

Molecular contrast agents (MCAs) are generally referred to the organic small-molecule chromophores. They usually exhibit distinct and characteristic absorption peak(s) due to their well-defined chemical structures, which are favourable for spectral unmixing. Most of them are of conjugated systems with delocalized electrons based on the aromatic rings and/or double bonds, and can be chemically modified to optimize their photophysical, chemical and biological properties, such as optical absorption, solubility, chemo/photostability and targeting ability. In addition, they raise fewer toxicity concerns compared to other types of contrast agents, especially inorganic ones, since MCAs are usually excreted quickly from the body *via* the liver or renal clearance pathway. Among numerous MCAs, indocyanine green (ICG, with its maximum absorbance at 790 nm) and methylene blue (MB, with its maximum absorbance at 670 nm) have been approved by the Food and Drug Administration (FDA) for clinical use (Fig. 3a). To date, a number of new biomedical applications have been achieved by using MCAs.[30–35]

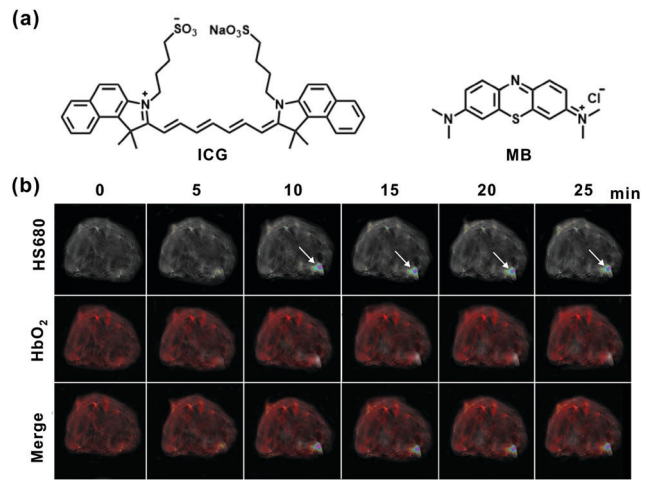

Fig. 3 (a) Chemical structure of the FDA-approved MCAs (ICG and MB). (b) Evaluation of accumulation of HS680 by breast tumor tissue *via* multispectral optoacoustic imaging. White arrow indicates the presence of HS680 (displayed in color) in tumor, which is overlaid onto the grayscale single-channel (900 nm) background image. Reproduced from ref. 30 with permission Elsevier copyright 2018.

Pharmacokinetics is an important parameter used to study the movement of foreign substances (mostly the drugs) into, through and out of an organism, which includes the processes of liberation, absorption, distribution, metabolization and excretion. Recently, Xiao *et al.* utilized MSOT to investigate the pharmacokinetics of HypoxiSense 680 (HS680), a commercially available and tumor-targeted MCA, in a mouse xenograft model of breast cancer (Fig. 3b).[30] In addition, Lavaud *et al.* used a new MCA (Angiostamp800) with tumor-targeting specificity to noninvasively monitor the liver metastasis progression *in vivo*.[31] They demonstrated that, the more advanced the metastasis development, the higher the optoacoustic signal generated, suggesting that this strategy may be used for precisely discriminating the disease stages and healthy state in mice.

Notably, the chromophores with quite low fluorescence quantum yields are termed as dark (or black hole) quenchers, and some of them are commercially available and have been employed in many fields. Some dark quenchers possessing high absorption in the near-infrared region are particularly suitable for multispectral optoacoustic imaging. Roberts *et al.* developed a novel MCA (QC1-pHLIP) by incorporating a targeting peptide into a commercial dark quencher QC1.[32] Using MSOT, the QC1-pHLIP could distinguish healthy tissues from breast cancer tissues *in vivo* with a high signal-to-noise ratio (SNR), thus demonstrating the QC1-pHLIP's potential in imaging-guided surgical applications. In another research, Haedicke *et al.* developed an MCA named BHQ-1-cRGD by attaching another commercial black hole quencher 1 (BHQ-1) with a targeting peptide and achieved the specific optoacoustic detection of glioblastoma tumors *in vitro* as well as *in vivo*.[33]

Apart from the commercialized MCAs, many functional MCAs with new chemical structures have also been successfully developed and applied in multispectral optoacoustic imaging during recent years. For example, β-cells control the secretion of insulin, and β-cell dysfunction leads to diabetes. Since glucagon-like peptide-1 receptors (GLP-1R) are abundant on the β-cell surface, Roberts *et al.* synthesized an MCA ($E4_{x12}$-Cy7) by conjugating a GLP-1R-targeted peptide (an exendin-4 analog) to a NIR chromophore Cy7 *via* click chemistry, and used it for the MSOT imaging of β-cells. This strategy may provide a new approach for monitoring diabetes and its progression.[34] Moreover, Kim *et al.* designed a molecular dye named TiNIR for the detection of tumor-initiating cells (TIC) in human lung tumors through MSOT/fluorescence imaging.[35]

Despite recent promising progresses, MCAs also exhibit some disadvantages, such as lower molar extinction coefficients, being prone to photobleaching and the tendency to aggregate in aqueous media. These issues should be addressed by a strategical design of the chemical structure of the chromophores in the future work. Still, MCAs have shown great potential for future applications as contrast agents due to some immanent merits such as well-defined molecular structure, versatility in structural design, as well as flexibility in the

modification of optical properties, which are favorable for the development of robust contrast agents including the activatable ones.

4.2 Nanosized contrast agents (NCAs)

Nanosized contrast agents (nanoagents) are currently the largest category of exogenous contrast agents and can be subdivided into inorganic metallic nanoagents, inorganic non-metallic nanoagents and organic nanoagents, based on the nature of signalling chromophores (Fig. 4a–c). Thanks to their high molar extinction coefficients, these nanoagents typically generate stronger optoacoustic signals compared to MCAs, and they can be fabricated into nanostructures of different sizes and shapes. Unlike small-molecule counterparts which are obtained by chemical synthesis, NCAs are usually prepared *via* physical interactions and/or chemical reactions between the chromophore(s) and non-chromophore(s), and sometimes multifunctionality can be achieved, such as multi-mode bioimaging and theranostics.

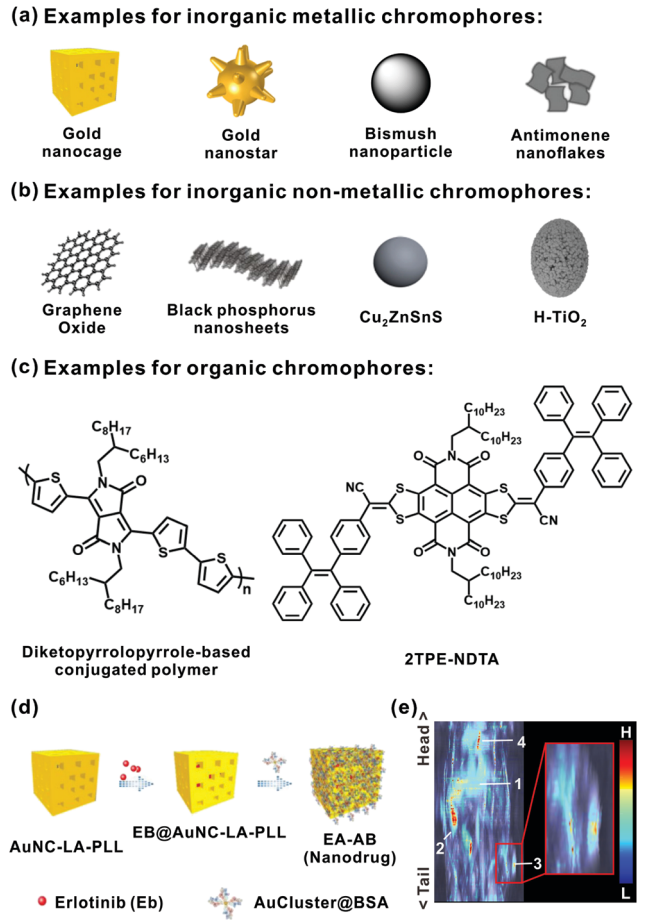

Fig. 4 Examples of inorganic metallic (a), inorganic non-metallic (b) and organic (c) chromophores. (d) Fabrication of an Au nanocage-based NAC (EA-AB). (e) The *x*–*z* 2D overview multispectral optoacoustic images of tumor-bearing mice after tail-vein injection of EA-AB. The biodistribution of EA-AB in mice at 4 h post-injection is demonstrated in the rainbow color, which is overlaid onto the grayscale single-channel (800 nm) background image of the anatomical information. Organ labeling: (1) liver; (2) spleen; (3) tumor; (4) lung. Panels (d) and (e) reproduced from ref. 37 with permission from Wiley-VCH copyright 2019.

4.2.1 Inorganic metallic nanoagents. Metallic nanoagents mainly comprise some metal-based nanostructures, which exhibit intense absorbance bands and high photothermal conversion efficiency due to the localized surface plasmon resonance (LSPR) effect.[36] The LSPR is a phenomenon in which the conduction electrons in the metal nanostructures oscillate relative to the core when exposed to the light of an appropriate wavelength. A substantial part of the oscillation energy is converted into heat, which accounts for the excellent contrast of metallic nanostructures in optoacoustic imaging. Importantly, the frequency of the LSPR determines the wavelength of their peak absorption, which can be tuned by changing the composition, geometry, size, separation distance and dielectric environment of the nanostructures.[36] This makes it possible to obtain the desirable metallic nanostructures with an ideal optoacoustic performance by simply changing the preparation method. Notably, the metallic nanoagents generally need to be modified with functional molecules or structures to improve their water dispersibility and biocompatibility, as well as to endow some favourable properties such as targeting and therapeutic capabilities.

In 2019, Zhan *et al.* reported a gold nanocage (AuNC)-based nanodrug (EA-AB) for imaging and tumor inhibition (Fig. 4d).[37] In this hybrid gold nanostructure, AuNC served as the drug carrier, the contrast agents for multispectral optoacoustic imaging, as well as the PTT generator. The tumor biodistribution and metabolic process could be visualized and tracked *via* whole-body MSOT imaging in a spatiotemporal manner. Also, the nanodrug exhibited significant antitumor efficacy *in vivo*.

Other gold nanostructures can also be employed to fabricate nanoagents. In 2018, Neuschmelting *et al.* reported a hybrid nanoagent composed of a gold nanostar core and a polyethylene glycol (PEG)-coated and IR780-embedded silica shell.[38] With strong absorption in the 700–900 nm range, the gold nanostar core acting as the contrast agent enabled the imaging of the brain glioblastoma. In another study, Jiang *et al.* engineered a glutathione-coated Au_{25} nanocluster system with strong NIR absorption and high renal clearance capability, which served as an exogenous contrast agent for visualizing and tracking its metabolism in kidneys.[39]

In addition to gold, some other metals have recently been exploited to form contrast agents. Yang *et al.* recently designed and fabricated a bismuth (Bi)-based multifunctional nanoagent (Bi@DLPC).[40] The strong absorption in the NIR region and the high atomic number (83) of bismuth contribute to the excellent photothermal conversion and OA/CT imaging performances, which display great potential for disease imaging in clinical trials.

Moreover, Yu *et al.* prepared the liquid-phase exfoliated antimonene nanoflakes as an extraordinary exogenous contrast agent.[41] Antimonene showed excellent contrast owing to its high molar extinction coefficient and high photothermal conversion efficiency resulting from its low thermal conductivity, high interfacial thermal conductivity, and lack of photon emission.

Such an exceptional optoacoustic performance allowed the *in vitro* monitoring of intracellular events and *in vivo* imaging of tumours in animal models.

4.2.2 Inorganic non-metallic nanoagents. Inorganic non-metallic nanoagents can be further classified into elemental nanoagents and inorganic compound ones. The former includes carbon nanostructures (such as nanotubes and graphenes), black phosphorus-based nanostructures, boron nanosheets, *etc.*, and the latter includes various inorganic oxides, sulphides, selenides, *etc.* This class of nanostructures can be readily engineered to possess strong absorption in the near-infrared range with high photostability, and they can also be covalently or noncovalently functionalized with various materials for diverse biomedical applications.

Chang *et al.* developed a nanoagent (GO/$MnWO_4$/PEG) with little *in vivo* toxicity through the *in situ* growth of $MnWO_4$ nanoparticles onto the surfaces of graphene oxide (GO) in the presence of PEG.[42] Compared to GO alone, GO/$MnWO_4$/PEG displayed significantly improved NIR absorbance, thus ensuring enhanced optoacoustic imaging performance. In addition, by adopting a simple mixing procedure, Guo *et al.* developed an inorganic non-metallic nanoagent (BPNS@TA–Mn) by coating a tannic acid (TA)–Mn^{2+} chelate onto black phosphorus nanosheets.[43] Due to its high NIR absorption and photothermal conversion capability, the BPNS@TA–Mn displayed not only excellent optoacoustic imaging performance, but also potent tumor inhibition ability as a result of the PTT effect.

Besides the elemental substances, a number of inorganic compounds have also been explored as contrast agents. For example, Tan *et al.* prepared bovine serum albumin-coated ultrasmall Cu_2ZnSnS_4 nanocrystals (CZTS@BSA) for the dual-mode imaging of tumors.[44] Their high absorption in the NIR range and longitudinal relaxivity made it an ideal exogenous signalling chromophore for MSOT and MR imaging. In addition, Wang *et al.* synthesized a multilayer core–shell structured nanocomposite (Fe@γ-Fe_2O_3@H–TiO_2) with full-spectrum absorption in the UV-vis-NIR region.[45] The H–TiO_2 shell served as the catalytic agent, photothermal agent and contrast agent for optoacoustic imaging, while the Fe@γ-Fe_2O_3 core played dual roles as the magnetic-separation agent and the magnetic-targeted agent. This multifunctional nanocomposite achieved MR/PT/OA triple-mode imaging-guided photothermal therapy with enhanced efficacy in tumour inhibition.

Recently, Liu *et al.* also prepared biocompatible CuS nanoparticles with a broad absorption band covering both NIR-I and NIR-II biological windows.[46] They discovered that in multispectral optoacoustic imaging, the SNR of the CuS nanoparticles at 1050 nm was 1.5-fold higher than that at 700 nm in both phantom and *in vivo* tests. This strategy provided a non-invasive method to accurately monitor the retention and metabolism of the nanoparticles *in vivo*.

4.2.3 Organic nanoagents. Organic nanoagents can be divided into polymer nanoagents and small molecular ones. The polymer nanoagents generally refer to the semiconducting polymer nanoagents. These agents usually have a highly delocalized π-conjugated backbone and display an intense absorption band in the NIR range. Moreover, the modification of their backbones by adjusting the degree of polymerization or changing the electron-donating/-withdrawing ability of the substituted group enables the tuning of optical properties.[47]

For instance, Duan *et al.* developed a new nanoagent (CP-IO) for tumor imaging by encapsulating diketopyrrolopyrrole-based conjugated polymers (CP) and iron oxide nanoparticles into phospholipid vesicles.[48] Compared to bare CP nanoparticles, the hybrid nanoagent CP-IO exhibited a 45% amplification in optoacoustic signal intensity due to the additional heat generation and faster heat dissipation brought about by the iron oxide nanoparticles.

On the other hand, some small-molecule chromophores are water-insoluble and cannot be directly used as MCAs. However, they can be encapsulated into various carriers and then used as nanoagents. For example, Zhao *et al.* synthesized two molecular dyes (2TPE-NDTA and 2TPE-2NDTA) with strong NIR absorption, as well as low fluorescent emission, and encapsulated them into phospholipid vesicles.[49] The nanoagent displayed exceptional photothermal conversion due to the intramolecular motion-induced photothermy, and thereby achieved high-contrast optoacoustic imaging of tumors in a mouse model. In addition, Roberts *et al.* developed a library of NCAs based on biocompatible nanoemulsions (NEs) by encapsulating commercially available NIR chromophores into phospholipids.[20] Among the obtained nanoemulsions, NE-IRDye QC1 exhibited the highest optoacoustic signal, and enabled tumor visualization in a mouse model of breast cancer by MSOT imaging.

Interestingly, incorporating a small-molecule dye into a metal–organic framework (MOF) structure can also produce a nanoagent. Zhang *et al.* designed such a MOF structure (DBBC-UiO) based on the bacteriochlorin ligand as well as $Hf_6(\mu_3\text{-}O)_4(\mu_3\text{-}OH)_4$ clusters and used it as a novel nanosystem for optoacoustic imaging.[50] The DBBC-UiO displayed multiple absorption peaks in the vis-NIR region, which was conducive to multispectral optoacoustic imaging.

Moreover, the self-assembly process can be explored to form multifunctional nanoagents. Xing *et al.* fabricated a series of versatile nanosystems through the self-assembly of biliverdin, targeting peptides and different metal ions.[51] For these nanosystems, the biocompatible biliverdin with an intense NIR absorption favoured optoacoustic imaging and PTT, while the metal ions served as the contrast agent for complementary imaging.

In 2019, Fathi *et al.* also developed a biodegradable biliverdin-based NCA through nanoprecipitation.[52] The optoacoustic and spectral characteristics of the resultant biliverdin nanoparticles (BVNPs) could be tuned by changing the synthesis time and reaction media of the nanoprecipitation procedure. Importantly, the BVNPs could detect sentinel lymph nodes *in vivo* by optoacoustic imaging and be completely biodegraded by the biliverdin reductase in the body.

Even though the nanoagents typically have higher molar extinction coefficients, their relatively broad absorption spectra without characteristic peaks often impede spectral unmixing and thus might cause false signals. In addition, the nanosized contrast agents may cause prolonged accumulation and retention

in the reticuloendothelial system upon administration, which elicits toxicity and immune responses. Moreover, owing to their multiple components, the purification, quantification and synthesis reproducibility remain challenging.

4.3 Genetically engineered contrast agents (GECAs)

Genetically engineered contrast agents refer to the proteins which are expressed by reporter genes and can either directly generate optoacoustic signals or catalyse the production of chromophores that yields optoacoustic signals (Fig. 5a).[53] Compared to other exogenous contrast agents, GECAs have the unique advantage of *in situ* expressions over extended periods, thus allowing longitudinal studies. In addition, this strategy enables the visualization of the pathological processes of genetic disorders at the cellular or molecular level.

In 2019, Gujrati *et al.* reported a new strategy for contrast enhancement in optoacoustic imaging using bioengineered-bacterial outer-membrane vesicles (OMVs).[54] They fabricated the OMVs encapsulating biopolymer-melanin (OMV^{Mel}) by engineering msbB gene-inactivated *Escherichia coli* strain to overexpress a tyrosinase transgene which can manipulate the synthesis of melanin, as shown in Fig. 5b and c. Upon NIR light irradiation, the OMV^{Mel} generated strong optoacoustic signals for MSOT imaging, thereby achieving the non-invasive monitoring of the tumor-associated OMV^{Mel} distribution *in vivo*.

To achieve neuroimaging with the multispectral optoacoustic imaging technique, Gottschalk *et al.* devised a customized system for both *ex vivo* and *in vivo* imaging.[55] By using a genetically encoded calcium indicator GCaMP6f expressed in mice as a contrast agent, they could achieve the real-time 3D visualization of the stimulus-evoked slow hemodynamics, fast calcium transients across the brain and even the whole-brain neuronal activity.

Very recently, Morales *et al.* reported the use of gene-transfected *Lactococcus lactis* (*L. lactis*), a facultative anaerobic Gram-positive lactic acid bacterium, as a GECA for imaging tumour hypoxia.[56] Upon administration, *L. lactis* could target melanoma hypoxic niches and express β-galactosidase (β-Gal) or infrared fluorescent protein (IRFP713) for imaging. The latter could be directly visualized using MSOT imaging, while the former could catalyse its substrate 5-bromo-4-chloro-3-indolyl-β-D-galactopyranoside (X-gal) and produce a NIR chromophore with a characteristic absorption spectrum distinguishable from that of hemoglobin. As a result, the tumour hypoxia niches could be precisely mapped with MSOT imaging.

In recent years, it has been discovered that some fluorescent protein (FP)-like proteins with high extinction coefficients and negligible fluorescence quantum yields, called chromoproteins, are more suitable as contrast agents for optoacoustic imaging. Moreover, the optoacoustic performance of chromoproteins can be further improved through directed evolution and iterative screening methods. Using this strategy, Li *et al.* prepared two GECAs based on the chromoprotein variants cjBlue2 and tdUltramarine2 which displayed 2 to 4-fold increases in the

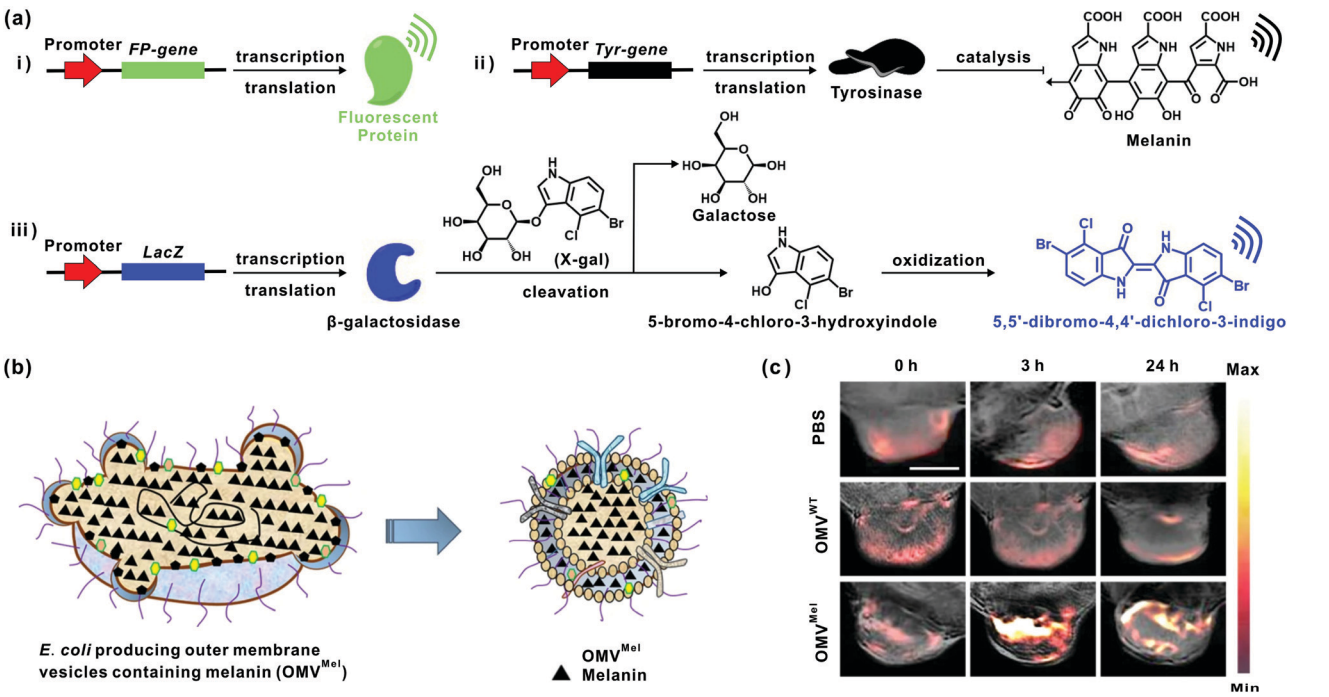

Fig. 5 (a) Genetically engineered contrast agents for multispectral optoacoustic imaging. (i) Genetically encoded production of fluorescent protein (FP) by FP gene. (ii) Genetically encoded production of melanin by tyrosine gene. (iii) Genetically encoded production of a blue chromophore 5,5-dibromo-4,4-dichloro-indigo by LacZ reporter gene and chromogenic agent X-gal. (b) Schematic representation of OMV^{Mel} purified after vesiculation from the parental bacteria. OMV, outer membrane vesicle. (c) 4T1 tumour-bearing mice were given a single injection of PBS or 150 μg of OMV^{WT} or OMV^{Mel} *via* the tail vein. Tumor-specific accumulation over time was monitored using a commercially available preclinical MSOT system. Panels (b) and (c) reproduced from ref. 54 with permission Springer Nature copyright 2019.

optoacoustic signal-to-noise ratio and enabled more accurate spectral unmixing in the ears of rats.[57]

Recent advances in the development of GECAs have undoubtedly provided a brilliant new approach for multispectral optoacoustic imaging at the molecular level. However, efforts are still needed to reasonably control the expression level of signalling chromophores, because excessively high expressions may affect the growth and metabolism of host cells, and even cause toxic effects and immune responses, which may eventually jeopardize the clinical transformation of GECAs.

5. Activatable contrast agents

The contrast agents introduced above can only generate unchanged optoacoustic signals upon excitation and are therefore referred to as "always on" contrast agents. These "always on" agents produce steady optoacoustic signals no matter whether they engage with or are in the vicinity of the target of interest (*e.g.*, disease site). Hence, they could cause strong background noise themselves and are unable to precisely reflect biological activities at molecular levels. On the other hand, the activatable contrast agents, also known as smart contrast agents, can generate variations in the photophysical properties (*e.g.*, absorption wavelength, absorption intensity, transformation of nonradiative relaxation or fluorescence quantum yield) of signalling chromophores in response to specific biological stimuli and subsequently elicit changes in optoacoustic signals. Notably, the variations in photophysical properties are typically caused by the alteration of the intramolecular electronic state, change in the intramolecular movement/rotation degree, transformation between the aggregate and non-aggregate states, *etc.* In contrast to "always on" contrast agents, the activatable ones can only be activated by specific biological stimuli (such as a change in the level of enzymes, ions, reactive oxygen/nitrogen species, pH, *etc.*) and display multiple advantages, such as low background noise and capability of the real-time tracking of biological dynamics. Herein, according to the signal variation modes of optoacoustic contrast agents upon activation, we divide them into three types: turn-off contrast agents, turn-on contrast agents and ratiometric contrast agents (Fig. 6a).

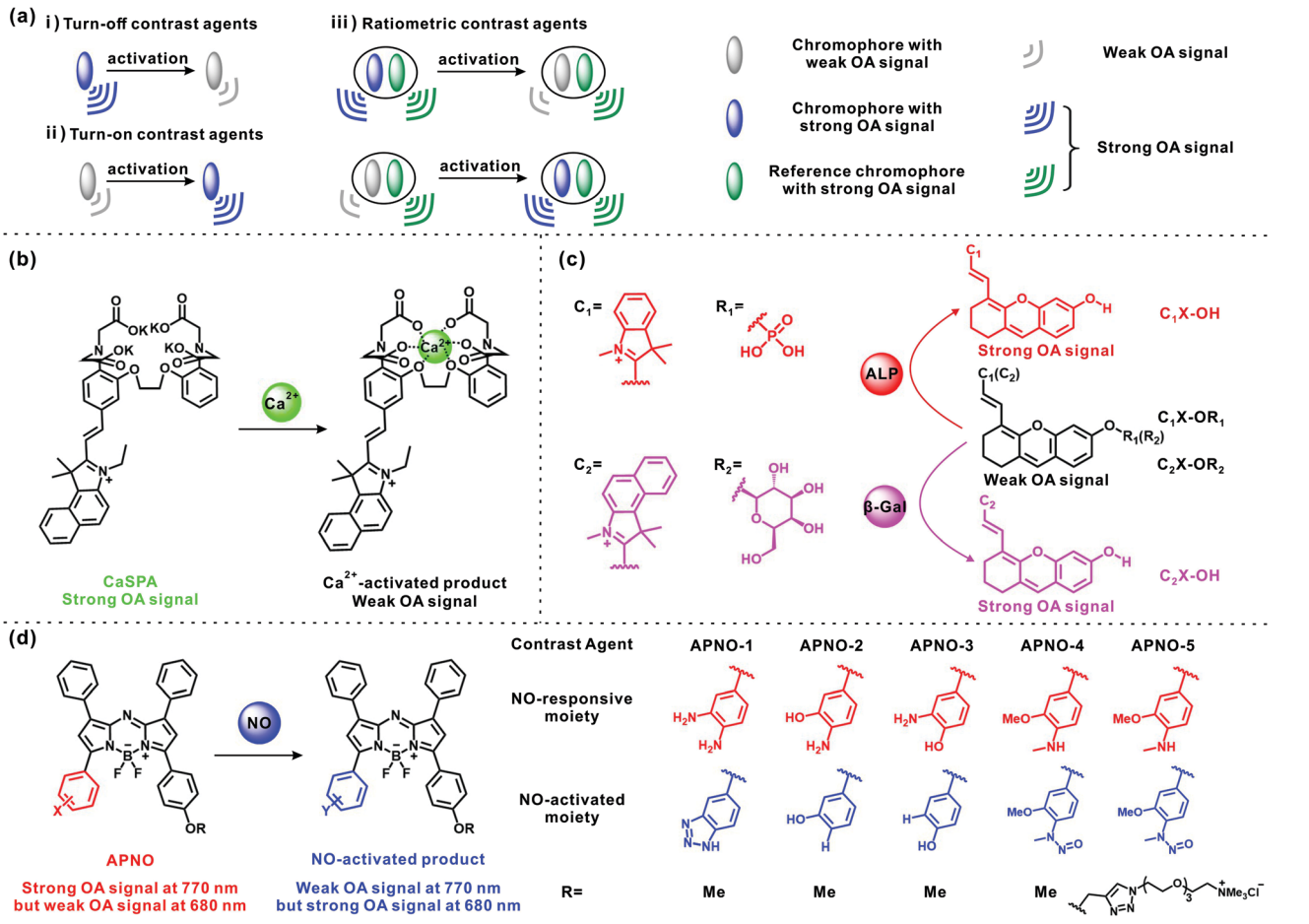

Fig. 6 (a) Schematic illustration for activatable contrast agents: (i) turn-off contrast agents, (ii) turn-on contrast agents and (iii) ratiometric contrast agents. (b) Illustration for structural change of a turn-off contrast agent CaSPA in response to Ca^{2+}. (c) Illustration for structural changes of two turn-on contrast agents in response to ALP and β-Gal, respectively. (d) Illustration for structural changes of a series of ratiometric agents (APNO) in response to NO.

5.1 Turn-off contrast agents

Turn-off contrast agents are those contrast agents which undergo a significant decrease in optoacoustic signal intensity after being activated by a specific biological stimulus. For instance, Roberts *et al.* demonstrated a metallochromic molecule, CaSPA, for the detection of calcium ions (Ca^{2+}) *in vitro* and *in vivo*.[58] The CaSPA could undergo a photo-induced charge transfer upon binding with Ca^{2+} and then induce a significant blue-shift in its absorption band, thereby causing a concomitant decrease in the optoacoustic signal intensity at the original wavelength (Fig. 6b). Furthermore, due to its high biocompatibility and cell permeability, CaSPA could be utilized for the multispectral optoacoustic imaging of intracellular Ca^{2+} transients in genetically unmodified cells, heart organoids and zebrafish larval brains.

In another study, Mishra *et al.* engineered a reversible optoacoustic contrast agent by including a Ca^{2+} chelating moiety into the cyclohexenyl ring linked with a NIR chromophore IR-780.[59] Upon the addition of Ca^{2+}, this agent exhibited a robust reduction in absorbance as a result of the chelation reaction, which caused a strong decrease in the optoacoustic signal. This strategy offered a new approach to create a series of metallochromic contrast agents for sensing-specific divalent cations in deep tissues.

5.2 Turn-on contrast agents

In contrast to turn-off contrast agents, the turn-on ones generate no or weak optoacoustic signals in their non-activated states, which causes low background noise. Only when they engage with or are in the propinquity of specific biomarkers, evident optoacoustic signals are given out, which leads to a higher signal-to-background ratio (SBR) and hence the improved sensitivity and resolution. In recent years, a series of turn-on optoacoustic contrast agents have been developed based on different response mechanisms.[60–67]

For example, Wu *et al.* demonstrated a hyaluronidase (HAase)-responsive nanoagent (TCHM@HA) *via* the self-assembly of a positively charged tricyanofuran-containing polyene (TCHM) chromophore and a negatively charged hyaluronan (HA).[60] The overexpressed HAase in tumor cells specifically degraded hyaluronan into small fragments and evoked the disruption of the nanosystem. As a result, the TCHM chromophores transformed from the aggregated state to the deaggregated state and exhibited enhanced absorbance at 882 nm, thereby generating intense optoacoustic signals upon light irradiation, which were used for the spatiotemporal diagnosing and mapping of orthotopic bladder tumors and tumor metastases in the lymphatic system using MSOT imaging.

In another study, the same group designed two activatable xanthene-based molecular contrast agents (C_1X-OR_1 and C_2X-$OR_{2)}$ for the imaging of disease-specific biomarkers (hepatic alkaline phosphatase (ALP) and β-galactosidase (β-Gal)), as shown in Fig. 6c.[61] The contrast agents C_1X-OR_1 and C_2X-OR_2 could be catalysed by ALP and β-Gal, respectively, to their activated forms (C_1X-OH and C_2X-OH) with red-shifted absorption bands, thus generating enhanced optoacoustic signals. The enhancement of both optoacoustic signals was caused by biomarker-mediated structural transformations with varied electronic states. By using MSOT imaging, the drug-induced liver injury and lymphatic metastases in mice could be precisely detected through the respective imaging of hepatic ALP and β-Gal activities with the two contrast agents.

To endow targetability for their contrast agent, Cai *et al.* developed an activatable contrast agent, MPC, by incorporating a peptide-conjugated chlorophyll with a macrophage targeting moiety mannose.[63] After being specifically recognized and internalized by macrophages, the MPC could be cleaved by caspase-1 in the *Staphylococcus aureus* (*S. aureus*)-infected macrophages, and the resulting MPC residues assembled into J-type aggregates. The aggregation induced a remarkable red-shift in the absorption spectrum and thus changed into an optoacoustic signal, which enabled the detection of *S. aureus* infection *in vivo*.

In addition, An *et al.* developed a turn-on agent, Cu_2O, for colon cancer imaging.[65] After intravenous injection, the Cu_2O agent with weak absorption in the NIR range could accumulate at the colon tumour site and react with endogenous H_2S to produce Cu_9S_8 *in situ*, which exhibited strong NIR absorption and generated intense optoacoustic signals for imaging.

The MOF can also be utilized to prepare activatable contrast agents. In 2019, Liu *et al.* reported a turn-on nanoagent denoted as AMP NRs, which was constructed by loading 2,2′-azino-bis(3-ethylbenzothiazoline-6-sulfonic acid) into a MOF (MIL-100), and coating them with poly(vinylpyrrolidone).[67] After being specifically activated by H_2O_2 and then amplified by low pH in a tumor microenvironment, the AMP NRs exhibited remarkably enhanced NIR absorption and produced intense optoacoustic signals for imaging.

5.3 Ratiometric contrast agents

A turn-off or turn-on contrast agent only produces single-channel optoacoustic signals for imaging, and sometimes the single-channel signal suffers from interferences from multiple sources of environmental factors, such as fluctuations in instrumental parameters, variations in local temperatures and the concentration of the contrast agent. However, the ratiometric strategy can largely bypass these issues owing to its self-calibration nature. The ratiometric detection can be realized through introducing an additional signal by adding an internal reference or by designing a signalling chromophore which exhibits wavelength shifts in the presence of specific biological stimuli. Therefore, measuring the ratio of two-channel optoacoustic signal intensities can lead to more accurate and precise analysis.

Boron-azadipyrromethene (aza-BODIPY) is a commonly used organic chromophore, which has high extinction coefficients in the NIR range and exhibits good photostability. Recently, Li *et al.* designed two activatable contrast agents (APC-1 and APC-2) based on aza-BODIPY for the detection of Cu^{2+}.[68] In the presence of Cu^{2+}, the recognition element (2-picolinic ester) in the agent structure was hydrolysed, thus

causing a 70 nm red-shift in the absorbance and subsequent changes in the ratio of the optoacoustic signal intensity at 697 and 767 nm, which realizes the ratiometric response towards Cu^{2+}.

Nitric oxide (NO) is an endogenous gasotransmitter and plays a vital role in many diseases including inflammation, infection and cancer.[69] Reinhardt *et al.* developed a series of NO-responsive contrast agents (APNO) by incorporating *o*-phenylenediamine, *o*-aminophenol or *N*-methylaniline (as the recognition element) into aza-BODIPY (Fig. 6d).[70] Among them, the APNO-5 agent, which has a responsive *N*-methylaniline group and a hydrophilic PEGylated tetraalkylammonium group in its structure, was found most optimal in the detection of endogenous NO in a mouse model of inflammation. In another study, the same group found that, by replacing the 1- and 7-position phenyl rings with thiophenes, the optimized contrast agent SR-APNO-3 exhibited a 30 nm red-shift in the absorption peak in comparison to the parent agent APNO-5.[71] Moreover, the steric relaxation led to a 1.1-fold increase in optoacoustic sensitivity, which allowed for enhanced ratiometric responses in an intramuscular inflammation model and an allograft murine breast cancer model.

In another study, Teng *et al.* designed a dual-stimuli responsive nanoagent (DATN) by encapsulating a NO-responsive molecule (NRM) and a NO-insensitive molecule (NIM) into Pluronic F127.[72] The weak electron acceptor benzo[*c*][1,2,5]thiadiazole-5,6-diamine in the NRM could be oxidized by NO to a stronger acceptor 5*H*-[1,2,3]triazolo[4,5-*f*]-2,1,3-benzothiadiazole under acidic conditions. As a result, the NRM dye displayed increased absorption in the range of 600–750 nm due to the intramolecular charge transfer process, while the DATN dye showed unchanged absorbance at 950 nm. Correspondingly, the nanoagent DATN could image the tumor region in a ratiometric manner by exhibiting an enhanced optoacoustic signal at 680 nm and a constant optoacoustic signal at 950 nm in response to the combined action of NO and acidity.

Apart from those for mere NO detection, the contrast agents for both NO generation and the detection of NO release have also been explored in recent years. Zhou *et al.* developed two photocontrolled NO donors/detectors (photoNOD-1 and photoNOD-2) by introducing an NO donor aryl *N*-nitrosamine into aza-BODIPY.[73] Upon NIR irradiation, they could release NO and simultaneously generate the signalling chromophore for monitoring NO release *in vivo* with multispectral optoacoustic imaging.

Very recently, Ai *et al.* developed a ratiometric contrast agent by the integration of two NIR small-molecule cyanine chromophores (HCy5 and Cy7) onto the surface of a synthetic nanoparticle, which was utilized for the simultaneous detection of $O_2^{\bullet-}$ and $ONOO^-$ by MSOT imaging.[74] Upon oxidative or/and nitrosative stimulation, HCy5 could respond to $O_2^{\bullet-}$ and then induce π-conjugation in Cy5, which elicits an absorption increase at 640 nm and the corresponding optoacoustic signal. On the other hand, the other dye, Cy7 (with distinct absorption at 780 nm), experienced a structural degradation by $ONOO^-$ and displayed a reduced absorption at 780 nm and the corresponding optoacoustic signal. Such opposite optoacoustic signal variations in response to oxidative and nitrosative stimulations contributed to precisely validating their complex dynamics as well as correlations with the redox-mediated pathophysiological procession *in vitro* and *in vivo*.

Matrix metalloprotease 2 (MMP-2) is an extracellular protease, which has been found to be overexpressed in many cancers and associated with tumor aggressiveness. Levi *et al.* prepared a ratiometric contrast agent by linking two commercially available chromophores (BHQ3 and Alexa750) with a cell-penetrating peptide which has an MMP-2-cleavable amino acid sequence in its structure.[75] In the absence of MMP-2, it showed two optoacoustic signals at 675 and 750 nm which correspond to the absorption maxima of BHQ3 and Alexa750, respectively. After the cleavage by MMP-2 in the culture solution with fibrosarcoma cells HT1080, the Alexa750 moiety diffused away, leaving the BHQ3 moiety (linked with the cell-penetrating peptide) remained in the cells, and as a result, only one optoacoustic signal at 675 nm was detected in the cells. Obviously, this strategy can be used in designing other activatable contrast agents for multispectral optoacoustic imaging in various biomedical applications just by changing the chromophores and peptide backbone.

In 2019, Peters *et al.* ingeniously used *Rhodobacter*, a kind of phototrophic purple bacteria, as an activatable reporter for the MSOT imaging of macrophage activities.[76] The chromophore bacteriochlorophyll (BChl) *a* in *Rhodobacter* exhibits two intense characteristic absorption peaks at 800 nm and 860 nm, which can be readily identified and discriminated from that of the endogenous contrast agent in the tissues *via* spectral unmixing. Upon being phagocytized and disintegrated by macrophages inside the tumor, the bacteria released BChl *a* which subsequently underwent aggregation and exhibited a gradually decreased absorption at 800 nm in the tumor edge, whereas the two absorption peaks (at 800 nm and 860 nm) remained unchanged in the tumor core. The ratiometric MSOT imaging using this phenomenon successfully revealed the heterogeneity of the tumor microenvironment.

In addition, Zhang *et al.* reported a ratiometric nanoagent for the optoacoustic imaging of miRNA in tumor tissues. The nanoagent was prepared by coating the cancer cell membrane onto dendritic mesoporous silica nanoparticles which were preloaded with DNA sequences bound by a NIR chromophore (IRDye 800CW)/quencher (IRDye QC-1) pair.[77] Once activated by the target miRNA, the IRDye 800CW could be disassembled from IRDye QC-1 with the aid of DNA fuel strands released in the acidic and GSH-rich tumor microenvironment, thus eliciting significant ratiometric changes in optoacoustic signals for miRNA detection in live mice.

As stated above, the activatable contrast agents are capable of translating biological dynamics to optoacoustic signals and even enabling the quantification of the biomarkers of biological events. With the aid of multispectral optoacoustic imaging, the real-time visualization with enhanced sensitivity, higher signal-to-noise ratio and three-dimensional information can be achieved by using these contrast agents.

6. Clinical applications of contrast agents

In addition to the rapid development of optoacoustic contrast agents and their widespread use in biomedical applications, major progress in the improvement of optics (*e.g.* laser source) and detectors (*e.g.* hand-held detector)[78] has also been made during the last few decades, which paves the way for the clinical applications of multispectral optoacoustic imaging. For clinical applications, currently, only endogenous absorbers (such as hemoglobin, lipids and collagens) and two FDA-approved exogenous contrast agents (ICG and MB) can be utilized for multispectral optoacoustic imaging. Indeed, in recent years, clinical applications have been achieved with multispectral optoacoustic imaging (Fig. 7).[26,79–83]

Lymphatic metastases occur in many early malignant tumors such as melanomas, and excision and subsequent histological analysis of sentinel lymph nodes (SLNs) are commonly used for the prognostication and determination of patient survival. Recently, Stoffels *et al.* employed MSOT imaging to detect several SLNs of patients by imaging melanin and administrated ICG *ex vivo* and *in vivo* (Fig. 7a–c).[79] For cancer-free SLN identification, MSOT imaging achieved 100% sensitivity and 48% to 62% specificity. This study offered a resolution that the SLN spots could be positioned, and a regular multispectral optoacoustic screening of patients determines the abnormal increase in melanin levels for assessing the likelihood of lymphatic metastases and guiding SLN excision.

Knieling *et al.* used MSOT imaging for the transabdominal evaluation of intestinal inflammation in 108 patients with Crohn's disease.[80] They determined the MSOT values corresponding to total hemoglobin, oxygenated hemoglobin (HbO_2), deoxygenated hemoglobin (Hb) and oxygen saturation in the intestinal walls of the patients with active Crohn's disease and patients with the nonactive disease. They found that there were significant differences between the active disease and nonactive disease for all the MSOT values except for oxygen saturation, suggesting that the intestinal-wall assessment by

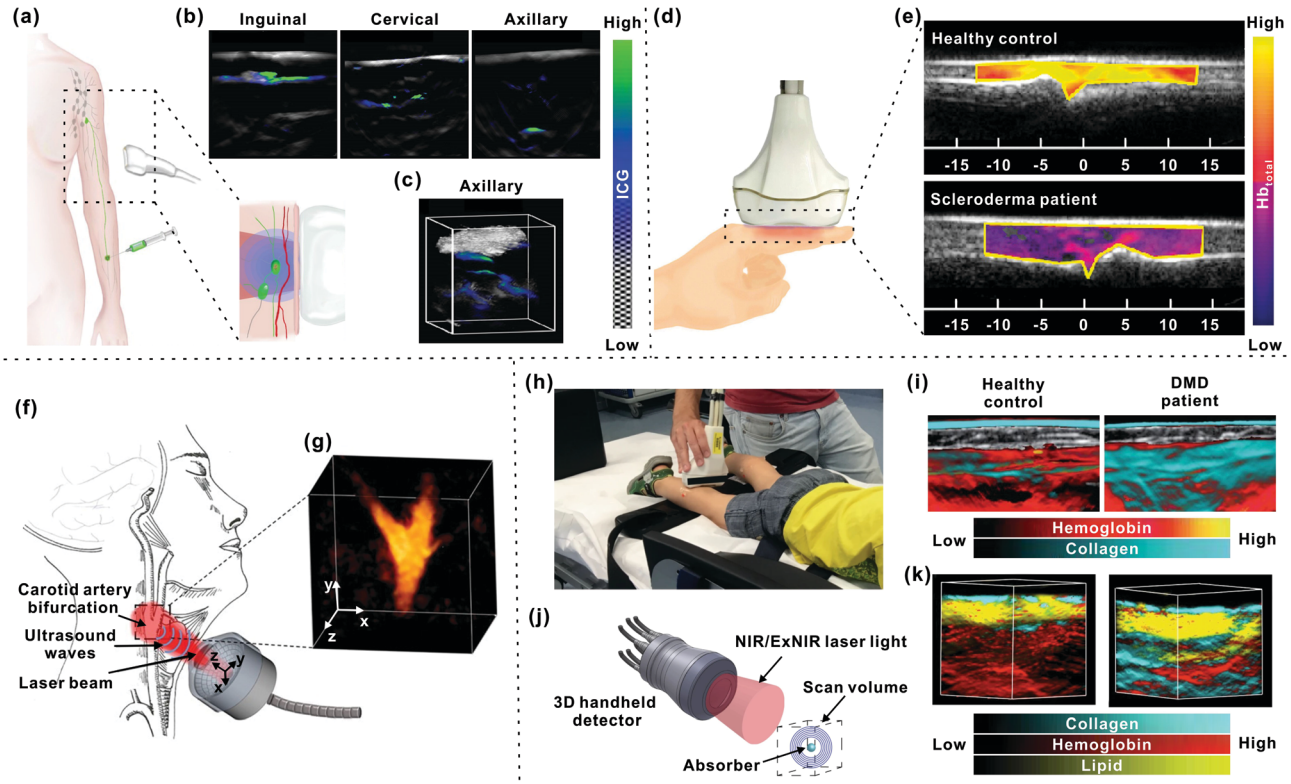

Fig. 7 Clinical applications of multispectral optoacoustic imaging. (a) Schematic illustration for detecting sentinel lymph nodes (SLNs) with MSOT imaging using an FDA-approved contrast agent ICG. (b) Representative 2D MSOT images of inguinal, cervical and axillary SLNs. (c) A 3D MSOT image of axillary SLNs. Panels (a)–(c) adapted from ref. 79 with permission from the American Association for the Advancement of Science copyright 2015. (d) Schematic illustration for the assessment of microvascular dysfunction in subcutaneous finger tissue of a patient with systemic sclerosis. (e) Representative MSOT images of total Hb in subcutaneous finger tissue of healthy volunteers or patients with systemic sclerosis. Panels (d) and (e) adapted from ref. 81 with permission from Wiley-VCH copyright 2018. (f) Schematic illustration for imaging carotid artery bifurcation area with a 3D detector. (g) A 3D view of reconstructed volumetric MSOT image of carotid bifurcation in a 44-year-old man. Panels (f) and (g) adapted from ref. 82 with permission from the Radiological Society of North America copyright 2019. (h) Schematic illustration for imaging the gastrocnemius muscle for detection of Duchenne muscular dystrophy (DMD) with a 2D detector. (i) Representative MSOT images of the gastrocnemius muscle from a 7-year-old healthy volunteer or a 5-year-old with DMD. (j) Schematic illustration for a handheld 3D hemispherical detector with a NIR (680–900 nm) or ExNIR (900–1100 nm) light source. (k) 3D MSOT images of the gastrocnemius muscle from the 7-year-old healthy volunteer or the 5-year-old with DMD by using the 3D detector. Panels (h)–(k) adapted from ref. 83 with permission from Springer Nature copyright 2019.

means of noninvasive MSOT imaging may distinguish remission from active disease in patients with Crohn's disease.

In another research, Masthoff *et al.* clinically evaluated the microvascular dysfunction in systemic sclerosis, which is an immune-mediated rheumatic disease, by imaging endogenous HbO_2 and Hb in the subcutaneous finger tissue of human hands by MSOT imaging.[81] They discovered that patients with systemic sclerosis displayed lower optoacoustic signals compared to the healthy controls (Fig. 7d and e).

In addition, Ivankovic and co-workers used a custom-designed volumetric MSOT system with a handheld detector to accomplish the real-time and three-dimensional visualization of the entire human carotid bifurcation area (Fig. 7f and g).[82] The carotid walls could be clearly displayed through imaging hemoglobin and a subsequent spectral unmixing at the periphery of the vessel lumen. Such an approach achieved the goal of simultaneously capturing the common carotid artery including the external carotid artery and internal carotid artery in a single volumetric image frame and providing real-time assessment of the anatomic and functional status of the human carotid artery.

In 2019, Regensburger *et al.* explored the endogenous collagens as a biomarker for the MSOT imaging of Duchenne muscular dystrophy (DMD),[83] which is a genetic disease that leads to muscle weakness and wasting over time. The illuminating muscle at multiple wavelengths enables the 3D MSOT imaging of collagens in pigs and pediatric human patients, thereby distinguishing the disease lesions from healthy ones (Fig. 7h–k). The MSOT data showed a steady increase in the optoacoustic signals of collagens in DMD over the time course, which is consistent with the histopathological results which show that muscular dystrophy and collagen formation all increase in diseased tissues. This clinical study indicates that the detection and quantification of endogenous collagens by MSOT imaging could provide a potential approach for monitoring disease progress in DMD (Fig. 7h–k).

7. Conclusions and outlook

By adopting multiwavelength excitation and spectral unmixing, multispectral optoacoustic imaging discriminates specific chromophore(s) from multiple contrast agents and absorbers in tissues, thus greatly increasing the detection sensitivity. In recent few years, a variety of new contrast agents have been developed and utilized in many biomedical fields covering (1) tumor identification, (2) organ function assessment, (3) vascular disease imaging, (4) brain research, (5) pharmacokinetic studies, (6) inflammation localization, (7) metabolism of adipose tissue observation, *etc.* Both endogenous (such as hemoglobin, melanin and lipids) and exogenous (chemical tools) contrast agents have been used for multispectral optoacoustic imaging. Exogenous contrast agents can be formed by organic small molecules, inorganic and organic nanostructures, or genetically engineered chromophores. Different types of contrast agents have their own pros and cons and one can select or design a suitable contrast agent for his/her specific purpose.

The high performance of multispectral optoacoustic imaging depends to a large extent on the interplay of the instrumentation/algorithm of the imaging system and the contrast agent used. However, as a newly emerged modality, continuous efforts have to be taken to achieve this goal. Among the currently available mainstream exogenous contrast agents, all nanosized and molecular ones have some drawbacks that impede highly sensitive imaging. Nanoagents exhibit high molar extinction coefficients and can correspondingly generate stronger optoacoustic signals, whereas their absorption bands are too broad for a multispectral system to obtain satisfactory sensitivity after unmixing. Moreover, there are some other challenges, such as circulation obstacles, off-target accumulation and lower tissue penetration efficiency, that can reduce the imaging sensitivity. Fortunately, a great number of chemical approaches are available nowadays to narrow the absorption bands to enhance the imaging sensitivity. For example, tight control over the uniformity of particle size can narrow their absorption bands.[84] Moreover, surface modification with targeting elements, as well as bio-conjugation/bio-functionalization, can promote the targeted accumulation of the agents, thereby enhancing the imaging sensitivity.[7]

On the other hand, the currently available molecular contrast agents exhibit narrow absorption bands conducive to spectral unmixing, but they are generally unable to afford intense imaging contrast and hence the high sensitivity owing to some of their optical characteristics such as lower molar extinction coefficients and higher quantum yields of competitive deactivation processes after excitation.[6] One solution is the molecular structural optimization, which includes the (1) adjustment of electron donor(s)/acceptor(s) in the chromophore to increase the extinction coefficient; (2) incorporation of rotor element(s) into an agent structure to enhance the intramolecular rotation and thereby increase the nonradiative decay, and (3) inclusion of a quencher moiety to eliminate fluorescence emission.[77] Another solution to this issue, as aforementioned, is to make the contrast agents activatable, by which the agents can respond to specific biological stimuli and produce changed optoacoustic signals, to reduce the interference from background signals and thereby achieve enhanced contrast. Indeed, a great number of existing NIR chromophores can be exploited to construct activatable contrast agents by following some well-established photophysical mechanisms such as photo-induced changes in intramolecular charge transfer or charge distribution.

On the other hand, for successful preclinical and clinical imaging, a multispectral optoacoustic imaging system should be compact and user-friendly and be able to provide real-time and high-resolution images at a depth limited only by the optical penetration depth of the light in the tissue probed.[14] Thus, the major components of a multispectral optoacoustic imaging system, such as the laser source, ultrasound detector, as well as spectral unmixing and image reconstruction algorithm, should be further optimized to meet the above requirement in future preclinical and clinical applications. For example, the pulsed laser source with strong pulse energy and optical parametric oscillators (OPOs) exhibits rapid wavelength-tuning

capability and high repetition rates, which is advantageous for multispectral imaging in preclinical research, but may not be suitable for small and portable systems. Moreover, in principle, the sensitivity can be increased by increasing the number of wavelengths of excitation light used in data acquisition and spectral processing, and this has been verified by a previous research study.[85] However, the more the wavelengths employed, the longer the time it takes to obtain the resulting images. Therefore, robust algorithms for spectral unmixing are needed to ameliorate the sensitivity and accuracy as well as to reduce the processing time, and some algorithmic unmixing approaches have been verified to display an increase in sensitivity.[19,20]

Another hurdle for the wide preclinical applications and clinical translations of multispectral optoacoustic imaging is the bulky and expensive devices (*e.g.* laser source) used in the imaging systems. One key to address this issue is the development of handheld systems. In recent years, much energy has been devoted to designing and developing handheld multispectral optoacoustic imaging systems.[78] However, further efforts have to be made before handheld systems can be more successfully used in both preclinical and clinical applications. First, the technical specifications of pulsed laser sources (*e.g.* size, cost, pulse length and energy) and detectors (*e.g.* size, sensitivity and array geometry), which are crucial for 2D and 3D handheld systems, should be drastically improved to better meet the requirement for imaging depth, sensitivity and resolution of both preclinical and clinical applications. In particular, 3D handheld systems exhibit unique real-time 3D imaging capabilities, and this is conducive to accelerating clinical observations and diagnosis; however, their accuracy, sensitivity and reliability of the acquired anatomical structural information in highly scattering and absorbing tissues at deep depths are lower than those of 2D systems,[86] and hence, further work on optics, electronics and ameliorated spectral unmixing algorithms would definitely enhance the performance of 3D systems. Second, the exogenous agents need to be further explored so that they can be better applied in 2D and 3D handheld systems. For example, an imaging depth of 4–5 cm has been achieved in human breast imaging *in vivo* with a 3D device.[87] However, this 4–5 cm depth may not be sufficient for imaging deep-seated organs like the human liver and intestine; this requires new improvement in their optical properties. In addition, the biocompatibility of the contrast agents should be further enhanced to suit biomedical applications, especially for clinical ones that require all the components of the exogenous agents to be approved by relevant authorities such as the FDA. As for the other issues concerning pharmacokinetics and targetability, they can be addressed by referring to the relevant strategies previously developed for other biomaterials, such that high-performance contrast agents can be obtained. With the development of more potent contrast agents and the miniaturization of optical and acoustic components, it has become possible to develop multispectral optoacoustic imaging systems that can be used in doctors' office, at patients' home and on battle grounds; and some other clinical applications, such as imaging-guided surgery, can be eventually achieved with great success.

It can be expected that the design and fabrication of robust contrast agents with excellent photophysical, chemical and biological properties will become a hotspot in the field of optoacoustic imaging. Notably, versatile applications for both preclinical and clinical research will also put forward rigorous demands on their properties, and thus accelerating the development of contrast agents. With the novel and robust contrast agents being further developed, multispectral optoacoustic imaging will find widespread applications in preclinical research, clinical transformation and public health services.

Conflicts of interest

There are no conflicts to declare.

Acknowledgements

This work was supported by the National Natural Science Foundation of China (21788102), the Fund of Guangdong Provincial Key Laboratory of Luminescence from Molecular Aggregates (2019B030301003), the Singapore Agency for Science, Technology and Research (A*STAR) AME IRG grant (A20E5c0081), and the Singapore National Research Foundation Investigatorship (NRF-NRFI2018-03).

Notes and references

1 A. V. Naumova, M. Modo, A. Moore, C. E. Murry and J. A. Frank, *Nat. Biotechnol.*, 2014, **32**, 804–818.
2 C. Balas, *Meas. Sci. Technol.*, 2009, **20**, 104020.
3 S. L. Jacques, *Phys. Med. Biol.*, 2013, **58**, R37–R61.
4 L. V. Wang and J. Yao, *Nat. Methods*, 2016, **13**, 627–638.
5 V. Ntziachristos and D. Razansky, *Chem. Rev.*, 2010, **110**, 2783–2794.
6 V. Gujrati, A. Mishra and V. Ntziachristos, *Chem. Commun.*, 2017, **53**, 4653–4672.
7 J. Weber, P. C. Beard and S. E. Bohndiek, *Nat. Methods*, 2016, **13**, 639–650.
8 J. Huang and K. Pu, *Angew. Chem., Int. Ed.*, 2020, **59**, 11717–11731.
9 C. Moore and J. V. Jokerst, *Theranostics*, 2019, **9**, 1550–1571.
10 Y. Liu, P. Bhattarai, Z. Dai and X. Chen, *Chem. Soc. Rev.*, 2019, **48**, 2053–2108.
11 H. J. Knox and J. Chan, *Acc. Chem. Res.*, 2018, **51**, 2897–2905.
12 C. J. Reinhardt and J. Chan, *Biochemistry*, 2018, **57**, 194–199.
13 M. D. Laramie, M. K. Smith, F. Marmarchi, L. R. McNally and M. Henary, *Molecules*, 2018, **23**, 2766.
14 G. Paltauf, R. Nuster and M. Frenz, *J. Appl. Phys.*, 2020, **128**, 180907.
15 L. V. Wang and S. Hu, *Science*, 2012, **335**, 1458–1462.
16 G. Paltauf, P. Hartmair, G. Kovachev and R. Nuster, *Photoacoustics*, 2017, **8**, 28–36.

17 A. Taruttis and V. Ntziachristos, *Nat. Photonics*, 2015, **9**, 219–227.
18 C. Lutzweiler and D. Razansky, *Sensors*, 2013, **13**, 7345–7384.
19 L. Ding, X. L. Déan-Ben, N. C. Burton, R. W. Sobol, V. Ntziachristos and D. Razansky, *IEEE Trans. Med. Imaging*, 2017, **36**, 1676–1685.
20 S. Roberts, C. Andreou, C. Choi, P. Donabedian, M. Jayaraman, E. C. Pratt, J. Tang, C. P. Medina, M. J. de la Cruz, W. J. M. Mulder, J. Grimm, M. Kircher and T. Reiner, *Chem. Sci.*, 2018, **9**, 5646–5657.
21 M. B. Karmacharya, L. R. Sultan, B. M. Kirkham, A. K. Brice, A. K. W. Wood and C. M. Sehgal, *Diagnostics*, 2020, **10**, 705.
22 I. Olefir, A. Ghazaryan, H. Yang, J. M. Najafabadi, S. Glasl, P. Symvoulidis, V. B. O'Leary, G. Sergiadis, V. Ntziachristos and S. V. Ovsepian, *Cell Rep.*, 2019, **26**, 2833–2846.
23 M. M. Costa, A. Shah, I. Rivens, C. Box, T. O'Shea, E. Papaevangelou, J. Bamber and G. T. Haar, *Photoacoustics*, 2019, **13**, 53–65.
24 J. Lavaud, M. Henry, J. L. Coll and V. Josserand, *Int. J. Pharm.*, 2017, **532**, 704–709.
25 S. Khattak, N. Gupta, X. Zhou, L. Pires, B. C. Wilson and Y. H. Yucel, *Exp. Eye Res.*, 2019, **179**, 157–167.
26 J. Reber, M. Willershäuser, A. Karlas, K. P. Yuan, G. Diot, D. Franz, T. Fromme, S. V. Ovsepian, N. Bézière, E. Dubikovskaya, D. C. Karampinos, C. Holzapfel, H. Hauner, M. Klingenspor and V. Ntziachristos, *Cell Metab.*, 2018, **27**, 689–701.
27 Y. Zhu, L. A. Johnson, Z. Huang, J. M. Rubin, J. Yuan, H. Lei, J. Ni, X. Wang, P. D. R. Higgins and G. Xu, *Biomed. Opt. Express*, 2018, **9**, 1590–1600.
28 Y. Yan, N. G. Lopez, M. Basij, A. V. Shahvari, F. V. Ortega, E. H. Andrade, S. S. Hassan, R. Romero and M. MehrMohammadi, *Biomed. Opt. Express*, 2019, **10**, 4643–4655.
29 H. Xiang, L. Zhao, L. Yu, H. Chen, C. Wei, Y. Chen and Y. Zhao, *Nat. Commun.*, 2021, **12**, 218.
30 T. G. Xiao, J. A. Weis, F. S. Gayzik, A. Thomas, A. Chiba, M. N. Gurcan, U. Topaloglu, A. Samykutty and L. R. McNally, *Photoacoustics*, 2018, **11**, 28–35.
31 J. Lavaud, M. Henry, P. Gayet, A. Fertin, J. Vollaire, Y. Usson, J.-L. Coll and V. Josserand, *Int. J. Biol. Sci.*, 2020, **16**, 1616–1628.
32 S. Roberts, A. Strome, C. Choi, C. Andreou, S. Kossatz, C. Brand, T. Williams, M. Bradbury, M. F. Kircher, Y. K. Reshetnyak, J. Grimm, J. S. Lewis and T. Reiner, *Sci. Rep.*, 2019, **9**, 8550.
33 K. Haedicke, C. Brand, M. Omar, V. Ntziachristos, T. Reiner and J. Grimm, *Photoacoustics*, 2017, **6**, 1–8.
34 S. Roberts, E. Khera, C. Choi, T. Navaratna, J. Grimm, G. M. Thurber and T. Reiner, *J. Nucl. Med.*, 2020, DOI: 10.2967/jnumed.120.252262.
35 J.-J. Kim, Y.-A. Lee, D. Su, J. Lee, S.-J. Park, B. Kim, J. H. J. Lee, X. Liu, S. S. Kim, M. A. Bae, J.-S. Lee, S. C. Hong, L. Wang, A. Samanta, H.-Y. Kwon, S.-Y. Choi, J.-Y. Kim, Y. H. Yu, H.-H. Ha, Z. Wang, W. L. Tam, B. Lim, N.-Y. Kang and Y.-T. Chang, *J. Am. Chem. Soc.*, 2019, **141**, 14673–14686.
36 E. Petryayeva and U. J. Krull, *Anal. Chim. Acta*, 2011, **706**, 8–24.
37 C. Zhan, Y. Huang, G. Lin, S. Huang, F. Zeng and S. Wu, *Small*, 2019, **15**, 1900309.
38 V. Neuschmelting, S. Harmsen, N. Beziere, H. Lockau, H.-T. Hsu, R. Huang, D. Razansky, V. Ntziachristos and M. F. Kircher, *Small*, 2018, **14**, 1800740.
39 X. Jiang, B. Du, S. Tang, J.-T. Hsieh and J. Zheng, *Angew. Chem., Int. Ed.*, 2019, **58**, 5994–6000.
40 C. Yang, C. Guo, W. Guo, X. Zhao, S. Liu and X. Han, *ACS Appl. Nano Mater.*, 2018, **1**, 820–830.
41 J. Yu, X.-H. Wang, J. Feng, X. Meng, X. Bu, Y. Li, N. Zhang and P. Wang, *Adv. Healthcare Mater.*, 2019, **8**, 1900378.
42 X. Chang, Y. Zhang, P. Xu, M. Zhang, H. Wu and S. Yang, *Carbon*, 2018, **138**, 397e409.
43 T. Guo, Y. Lin, G. Jin, R. Weng, J. Song, X. Liu, G. Huang, L. Hou and H. Yang, *Chem. Commun.*, 2019, **55**, 850–853.
44 L. Tan, J. Wan, W. Guo, C. Ou, T. Liu, C. Fu, Q. Zhang, X. Ren, X.-J. Liang, J. Ren, L. Li and X. Meng, *Biomaterials*, 2018, **159**, 108–118.
45 M. Wang, K. Deng, W. Lü, X. Deng, K. Li, Y. Shi, B. Ding, Z. Cheng, B. Xing, G. Han, Z. Hou and J. Lin, *Adv. Mater.*, 2018, **30**, 1706747.
46 Y. Liu, D. Gao, M. Xu and Z. Yuan, *J. Biophotonics*, 2019, **12**, e201800237.
47 L. Zhou, H. Zhou and C. Wu, *Wiley Interdiscip. Rev.: Nanomed. Nanobiotechnol.*, 2018, **10**, e1510.
48 Y. Duan, Y. Xu, D. Mao, W. H. Liew, B. Guo, S. Wang, X. Cai, N. Thakor, K. Yao, C.-J. Zhang and B. Liu, *Small*, 2018, **14**, 1800652.
49 Z. Zhao, C. Chen, W. Wu, F. Wang, L. Du, X. Zhang, Y. Xiong, X. He, Y. Cai, R. T. K. Kwok, J. W. Y. Lam, X. Gao, P. Sun, D. L. Phillips, D. Ding and B. Z. Tang, *Nat. Commun.*, 2019, **10**, 768.
50 K. Zhang, Z. Yu, X. Meng, W. Zhao, Z. Shi, Z. Yang, H. Dong and X. Zhang, *Adv. Sci.*, 2019, **6**, 1900530.
51 R. Xing, Q. Zou, C. Yuan, L. Zhao, R. Chang and X. Yan, *Adv. Mater.*, 2019, **31**, 1900822.
52 P. Fathi, H. J. Knox, D. Sar, I. Tripathi, F. Ostadhossein, S. K. Misra, M. B. Esch, J. Chan and D. Pan, *ACS Nano*, 2019, **13**, 7690–7704.
53 J. Brunker, J. Yao, J. Laufer and S. E. Bohndiek, *J. Biomed. Opt.*, 2017, **22**, 070901.
54 V. Gujrati, J. Prakash, J. M. Najafabadi, A. Stiel, U. Klemm, G. Mettenleiter, M. Aichler, A. Walch and V. Ntziachristos, *Nat. Commun.*, 2019, **10**, 1114.
55 S. Gottschalk, O. Degtyaruk, B. M. Larney, J. Rebling, M. A. Hutter, X. L. D. Ben, S. Shoham and D. Razansky, *Nat. Biomed. Eng.*, 2019, **3**, 392–401.
56 R. G. Morales, B. E. Rendon, M. T. Malik, J. E. G. Cabrales, A. Aucouturier, L. G. B. Humarán, K. M. McMasters, L. R. McNally and J. G. G. Gutierrez, *Cancers*, 2020, **12**, 438.
57 Y. Li, A. Forbrich2, J. Wu, P. Shao, R. E. Campbell and R. Zemp, *Sci. Rep.*, 2016, **6**, 22129.
58 S. Roberts, M. Seeger, Y. Jiang, A. Mishra, F. Sigmund, A. Stelzl, A. Lauri, P. Symvoulidis, H. Rolbieski, M. Preller,

X. L. D. Ben, D. Razansky, T. Orschmann, S. C. Desbordes, P. Vetschera, T. Bach, V. Ntziachristos and G. G. Westmeyer, *J. Am. Chem. Soc.*, 2018, **140**, 2718–2721.

59 A. Mishra, Y. Jiang, S. Roberts, V. Ntziachristos and G. G. Westmeyer, *Anal. Chem.*, 2016, **88**, 10785–10789.

60 Y. Wu, J. Chen, L. Sun, F. Zeng and S. Wu, *Adv. Funct. Mater.*, 2019, **29**, 1807960.

61 Y. Wu, S. Huang, J. Wang, L. Sun, F. Zeng and S. Wu, *Nat. Commun.*, 2018, **9**, 3983.

62 P. Anees, J. Joseph, S. Sreejith, N. V. Menon, Y. Kang, S. W.-K. Yu, A. Ajayaghosh and Y. Zhao, *Chem. Sci.*, 2016, **7**, 4110–4116.

63 Q. Cai, Y. Fei, L. Hu, Z. Huang, L.-L. Li and H. Wang, *Nano Lett.*, 2018, **18**, 6229–6236.

64 J. Ouyang, L. Sun, Z. Zeng, C. Zeng, F. Zeng and S. Wu, *Angew. Chem., Int. Ed.*, 2020, **59**, 10111–10121.

65 L. An, X. Wang, X. Rui, J. Lin, H. Yang, Q. Tian, C. Tao and S. Yang, *Angew. Chem., Int. Ed.*, 2018, **57**, 15782–15786.

66 Y. Huang, Y. Qi, C. Zhan, C. Zeng, F. Zeng and S. Wu, *Anal. Chem.*, 2019, **91**, 8085–8092.

67 F. Liu, L. Lin, Y. Zhang, Y. Wang, S. Sheng, C. Xu, H. Tian and X. Chen, *Adv. Mater.*, 2019, **31**, 1902885.

68 H. Li, P. Zhang, L. P. Smaga, R. A. Hoffman and J. Chan, *J. Am. Chem. Soc.*, 2015, **137**, 15628–15631.

69 Y. Wu, L. Sun, F. Zeng and S. Wu, *Photoacoustics*, 2019, **13**, 6–17.

70 C. J. Reinhardt, E. Y. Zhou, M. D. Jorgensen, G. Partipilo and J. Chan, *J. Am. Chem. Soc.*, 2018, **140**, 1011–1018.

71 C. J. Reinhardt, R. Xu and J. Chan, *Chem. Sci.*, 2020, **11**, 1587–1592.

72 L. Teng, G. Song, Y. Liu, X. Han, Z. Li, Y. Wang, S. Huan, X.-B. Zhang and W. Tan, *J. Am. Chem. Soc.*, 2019, **141**, 13572–13581.

73 E. Y. Zhou, H. J. Knox, C. J. Reinhardt, G. Partipilo, M. J. Nilges and J. Chan, *J. Am. Chem. Soc.*, 2018, **140**, 11686–11697.

74 X. Ai, Z. Wang, H. Cheong, Y. Wang, R. Zhang, J. Lin, Y. Zheng, M. Gao and B. Xing, *Nat. Commun.*, 2019, **10**, 1087.

75 J. Levi, S. R. Kothapalli, T.-J. Ma, K. Hartman, B. T. K. Yaku and S. S. Gambhir, *J. Am. Chem. Soc.*, 2010, **132**, 11264–11269.

76 L. Peters, I. Weidenfeld, U. Klemm, A. Loeschcke, R. Weihmann, K.-E. Jaeger, T. Drepper, V. Ntziachristos and A. C. Stiel, *Nat. Commun.*, 2019, **10**, 1191.

77 K. Zhang, X. Meng, Z. Yang, Y. Cao, Y. Cheng, D. Wang, H. Lu, Z. Shi, H. Dong and X. Zhang, *Adv. Mater.*, 2019, **31**, 1807888.

78 M. W. Schellenberg and H. K. Hunt, *Photoacoustics*, 2018, **11**, 14–27.

79 I. Stoffels, S. Morscher, I. Helfrich, U. Hillen, J. Leyh, N. C. Burton, T. C. P. Sardella, J. Claussen, T. D. Poeppel, H. S. Bachmann, A. Roesch, K. Griewank, D. Schadendorf, M. Gunzer and J. Klode, *Sci. Transl. Med.*, 2015, **7**, 317ra199.

80 F. Knieling, C. Neufert, A. Hartmann, J. Claussen, A. Urich, C. Egger, M. Vetter, S. Fischer, L. Pfeifer, A. Hagel, C. Kielisch, R. S. Görtz, D. Wildner, M. Engel, J. Röther, W. Uter, J. Siebler, R. Atreya, W. Rascher, D. Strobel, M. F. Neurath and M. J. Waldner, *N. Engl. J. Med.*, 2017, **376**, 1292–1294.

81 M. Masthoff, A. Helfen, J. Claussen, W. Roll, A. Karlas, H. Becker, G. Gabriëls, J. Riess, W. Heindel, M. Schäfers, V. Ntziachristos, M. Eisenblätter, U. Gerth and M. Wildgruber, *J. Biophotonics*, 2018, **11**, e201800155.

82 I. Ivankovic, E. Merčep, C.-G. Schmedt, X. L. D. Ben and D. Razansky, *Radiology*, 2019, **291**, 45–50.

83 P. Regensburger, L. M. Fonteyne, J. Jüngert, A. L. Wagner, T. Gerhalter, A. M. Nagel, R. Heiss, F. Flenkenthaler, M. Qurashi, M. F. Neurath, N. Klymiuk, E. Kemter, T. Fröhlich, M. Uder, J. Woelfle, W. Rascher, R. Trollmann, E. Wolf, M. J. Waldner and F. Knieling, *Nat. Med.*, 2019, **25**, 1905–1915.

84 H. D. Lu, B. K. Wilson, A. Heinmiller, B. Faenza, S. Hejazi and R. K. Prud'homme, *ACS Appl. Mater. Interfaces*, 2016, **8**, 14379–14388.

85 S. Tzoumas, A. Nunes, N. C. Deliolanis and V. Ntziachristos, *J. Biophotonics*, 2015, **8**, 629–637.

86 V. Neuschmelting, N. C. Burton, H. Lockau, A. Urich, S. Harmsen, V. Ntziachristos and M. F. Kircher, *Photoacoustics*, 2016, **4**, 1–10.

87 M. Klosner, G. Chan, C. Wu, D. F. Heller, R. Su, S. Ermilov, H. P. Brecht, V. Ivanov, P. Talole, Y. Lou, M. Anastasio and A. Oraevsky, *Proc. SPIE*, 2016, **9708**, 97085B.